

# Control of robot under sliding conditions and high speed

Philippe Martinet<sup>1</sup>, Roland Lenain<sup>2</sup>, Benoit Thuilot<sup>1</sup>, Michel Berducat<sup>2</sup>

<sup>1</sup> LASMEA, 24, av. des Landais, 63177 Aubière Cedex France

<sup>2</sup> Cemagref – Unité TSCF, 24 av. des Landais, BP 50085, 63172 Aubière Cedex. France.

---

## Abstract

Accurate control of high-speed mobile robots moving off-road constitutes a challenging robotic issue: numerous time-varying dynamic phenomena (and first of all, sliding effects) are no longer negligible and must explicitly be taken into account in control design, in order to ensure high accuracy path tracking. Since these phenomena are hardly measurable at a reasonable cost, they have to be estimated on-line. A multi-model based observer is here proposed, in order to supply on-line tire cornering stiffnesses (i.e. grip conditions) as well as mobile robot sideslip angles. It takes part of the complementarity between kinematic and dynamic mobile robot models, in order to significantly decrease the number of required robot inertial parameters (since their values are sometimes difficult to obtain). Full scale experiments demonstrate that the proposed observer can supply reactive and reliable sideslip angle estimates, so that high accuracy path tracking can still be achieved, whatever grip conditions and vehicle velocity.

---

## 1. Introduction

The increasing number of off-road robots in various fields of application appears as interesting solutions to arising social needs. From transportation to agricultural operations [2] (not to mention exploration, surveillance, military activities, etc.), many potential applications can take benefits of innovations in this area, increasing work accuracy or decreasing the level of risk (see [13]). Nevertheless, the complexity of the phenomena encountered off-road (linked to unpredictable interactions with the environment, [9]) requires the design of advanced control algorithms, especially when high-speed operations are desired. In particular, the accurate motion control of fast mobile robots in this context needs important development, since classical algorithms ([10]), designed initially for urban vehicles, leads to an unsatisfactory accuracy (as many interactions are neglected). As a result, the nonnegligible mobile robot dynamics has to be taken explicitly into account in the control process. If modeling techniques (see for instance [5]) permit to describe these complex interactions, they remain hardly tractable for control purpose, since numerous parameters have to be known (and are subject to change in off-road conditions). As an alternative, some approaches consider such phenomena as perturbations (see [14] for instance) to be rejected by robust techniques (as investigated in [4], [6], or [8]). However, these approaches tend to be conservative, even at limited speed, leading to an oscillating behavior.

A different approach has been proposed in previous work (see [7]), relying on an extended kinematic representation. Similar to the celebrated Ackermann model, it takes grip conditions into account thanks to the integration of sideslip angles, estimated on-line via an observer designed from this model. The model relevancy is then ensured and an adaptive control technique, coupled with a predictive action, then permits to control robot motion with a high accuracy (within  $\pm 10\text{cm}$ ) whatever ground conditions and the shape of the path to be followed. Nevertheless, the use of a sole kinematic representation does not allow to address satisfactorily high speed (above 10 km/h), since neglected dynamics introduce some delay in sideslip angle estimation. Therefore, in order to enable a significant increase in vehicle velocity (40km/h is expected in a near future), dynamic effects have to be accounted in sideslip angle observer.

In this paper, a new sideslip angle observer is proposed, mixing kinematic and dynamic models, in order to reduce estimation delays by accounting dynamic effects without considering numerous inertial parameters. It is composed of several steps, and relies firstly on the previous extended kinematic observer. Based on this preliminary estimation, an on-line adaptation of cornering stiffnesses, representative of grip conditions, can be proceeded, enabling the use of a dynamic model. Then a second sideslip angle observer using such a dynamic model is then implemented, allowing a more reactive estimation. These new estimated angles can then be introduced into the adaptive and predictive control laws, enabling an improved behavior. The proposed algorithm is detailed in a second part, after having recalled previous work (modeling, preliminary observer, and the unchanged control law formalism). Finally, experimental results are then reported to validate the efficiency of the proposed algorithm.

## 2. Mobile Robot Control

### 2.1. Extended kinematic model

Classical models used in path tracking applications basically rely on the rolling without sliding assumption, which is not applicable off-road. The direct use of such control laws indeed leads to large tracking errors, due to neglected dynamics (mainly low grip conditions, actuator delays and vehicle inertia). In order to design an accurate path tracking algorithm dedicated to off-road mobile robots acting

at high speed (several m/s), these specific phenomena must be taken into account. Dynamic representations permit to accurately describe such interactions, but they demand for so many parameters that they are hardly tractable for control purpose.

Consequently, the path tracking control law considered in this paper is designed from an alternative "extended kinematic model". This representation, detailed in [7], consists in adding a limited number of variables representative of low grip conditions into a pure kinematic model. As depicted in Figure 1, the two sideslip angles  $\beta_F$  and  $\beta_R$  (denoting the

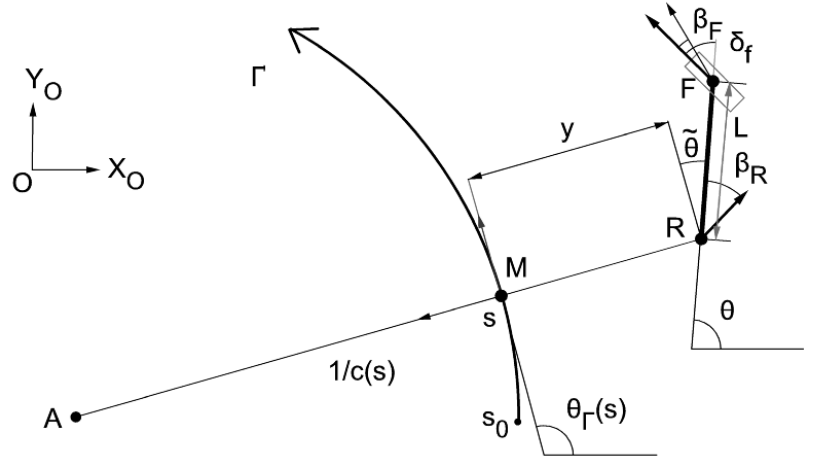


Figure 1: Path tracking parameters

difference between tire direction and actual speed vector orientation) have been introduced into a bicycle representation of the mobile robot as in [12]. Notations, depicted on Figure 1, are listed below.

- $F$  and  $R$  are respectively the center of the front and rear axle, where are located the virtual wheels of the bicycle model.  $R$  is the point to be controlled.
- $L$  is the vehicle wheelbase.
- $\theta$  is the orientation of vehicle centerline with respect to an absolute frame  $[O, X_O, Y_O]$ .
- $v$  is the vehicle linear velocity at point  $R$ , assumed to be strictly positive and manually controlled.
- $\delta_F$  is the front steering angle. It constitutes the control variable.
- $\beta_F$  and  $\beta_R$  are the front and rear side slip angles.
- $M$  is the point on the path  $\Gamma$  to be followed, which is the closest to  $R$ .  $M$  is assumed to be unique.
- $s$  is the curvilinear abscissa of point  $M$  along  $\Gamma$ .
- $c(s)$  is the curvature of the path  $\Gamma$  at point  $M$ .
- $\theta_\Gamma(s)$  is the orientation of the tangent to  $\Gamma$  at point  $M$  with respect to the absolute frame  $[O, X_O, Y_O]$ .
- $\bar{\theta} = \theta - \theta_\Gamma$  is the vehicle angular deviation with respect to  $\Gamma$ .
- $y$  is the vehicle lateral deviation at point  $R$  with respect to  $\Gamma$ .

In the following of the paper, the position and the orientation of the mobile robot is supposed to be measured, as well as the yaw rate and the velocity, thanks to on-board exteroceptive sensors (see section IV). Moreover, an angular sensor permits to measure the steering angle  $\delta^F$ . As a result, all the variables described above except sideslip angles  $\beta_F$  and  $\beta_R$  can be known (by measurement or preliminary calibration). Using the above notations, the mobile robot motion, expressed with respect to  $\Gamma$ , can be described by the set of equations (1), established in the non-sliding case in [11] and extended in [7] to account for the wheel skidding. The singularity when  $y = \frac{1}{c(s)}$  (i.e. when points  $R$  and  $A$  are superposed) is not encountered in practice, since the lateral deviation remains smaller than the radius of curvature of  $\Gamma$ .

$$\begin{cases} \dot{s} &= v \frac{\cos(\bar{\theta} + \beta_R)}{1 - c(s)y} \\ \dot{y} &= v \sin(\bar{\theta} + \beta_R) \\ \dot{\bar{\theta}} &= v [\cos(\beta_R)\lambda_1 - \lambda_2] \end{cases} \quad (1)$$

$$\text{with: } \lambda_1 = \frac{\tan(\delta_F + \beta_F) - \tan(\beta_R)}{L}, \lambda_2 = \frac{c(s) \cos(\bar{\theta} + \beta_R)}{1 - c(s)y}$$

## 2.2. Preliminary sideslip angle observation

Model (1) can accurately describe mobile robot motion, as soon as the two additional variables ( $\beta_F$  and  $\beta_R$ ) are properly known. The observation of these variables constitutes the core of this paper. Nevertheless, the preliminary observer defined in [7] is first recalled. It is based on the extended kinematic model (1) and supplies satisfactory results when mobile robots move at limited speed. The set of equations (1) can be rewritten into the state space form:

$$\begin{aligned}\dot{X}_{obs} &= f(X_{obs}, \delta_F, u) \\ &= \begin{cases} v \sin(\bar{\theta}_{obs} + u_2) \\ v \left[ \frac{\cos(u_2)[\tan(\delta_F + u_1) - \tan(u_2)]}{L} - \frac{c(s) \cos(\bar{\theta}_{obs} + u_2)}{1 - c(s)y_{obs}} \right] \end{cases}\end{aligned}\quad (2)$$

where  $X_{obs} = [y_{obs} \bar{\theta}_{obs}]^T$  is the observed state and  $u = [u_1 \ u_2]^T = [\beta_F \ \beta_R]^T$  is the sideslip angles to be estimated, viewed as a control vector to be designed in order to impose the convergence of  $X_{obs}$  to the measured state  $X_{mes} = [y_{mes} \bar{\theta}_{mes}]^T$ .

As sideslip angles do not exceed few degrees in practice, this state equation can be linearized with respect to the control vector  $u$  in the vicinity of zero (i.e. no sliding). It leads to:

$$\dot{X}_{obs} = f(X_{obs}, \delta_F, 0) + B(X_{obs}, \delta_F)u \quad (3)$$

with  $B(\dots)$  denoting the derivative of  $f$  with respect to  $u$ , evaluated at  $u = (0,0)$ :

$$B(X_{obs}, \delta_F) = \begin{bmatrix} 0 & v \cos(\bar{\theta}_{obs}) \\ \frac{v}{L \cos^2 \delta_F} & v \frac{c(s) \sin(\bar{\theta}_{obs})}{1 - c(s)y_{obs}} - \frac{v}{L} \end{bmatrix} \quad (4)$$

Provided that  $\bar{\theta}_{obs} \neq \frac{\pi}{2} [\pi]$  and  $v \neq 0$ , the matrix  $B$  is invertible. Let  $e = X_{obs} - X_{mes}$  be the observed error. Then an exponential convergence  $\dot{e} = Ge$  can be obtained by choosing:

$$u = B(X_{obs}, \delta_F)^{-1} (Ge + \dot{X}_{mes} - f(X_{obs}, \delta_F, 0)) \quad (5)$$

$G$  has to be chosen as an Hurwitz matrix and constitutes the observer gain imposing the settling times for the observed state. Since convergence of the observed state to the measured one has been achieved,  $u$  can be regarded as a relevant estimation of the sideslip angles.

### 2.3. Adaptive and predictive control law

The extended kinematic model (1), coupled with the preliminary observer (6), allows an accurate description of mobile robots behavior in off-road conditions. Furthermore, since a kinematic structure has been preserved, it offers interesting properties from a control design point of view, namely it can be converted into chained form, see [11]. The control law proposed in [7] consists in two steps: (i) an adaptive control law ensuring the convergence of the tracking error to zero and (ii) a predictive curvature servoing, which compensates for steering actuator delays.

The adaptive layer is based on the exact conversion of model (1) into chained form. Then a classical PID control is proposed for the auxiliary inputs in order to ensure the convergence of the actual lateral deviation to zero. The reverse transformation provides finally the non-linear expression (6) for the steering control law.

$$\delta_F = \arctan \left( \tan(\beta_R) + \frac{L}{\cos(\beta_R)} \left( \frac{c(s) \cos \bar{\theta}_2}{\alpha} + \frac{A \cos^3 \bar{\theta}_2}{\alpha^2} \right) \right) - \beta_F \quad (6)$$

with:

$$\begin{cases} \bar{\theta}_2 &= \bar{\theta} + \beta_R \\ \alpha &= 1 - c(s)y \\ A &= -K_p y - K_d \alpha \tan \bar{\theta}_2 + c(s) \alpha \tan^2 \bar{\theta}_2 \end{cases} \quad (7)$$

In addition to this non-linear control expression, a Model Predictive Control is applied to address specifically curvature servoing in expression (6). The steering control law can indeed be split into two additive terms:

$$\delta_F = \delta_{Traj} + \delta_{Deviation} \quad (8)$$

where  $\delta_{Deviation}$  is a term mainly concerned with errors and sliding compensation, while  $\delta_{Traj}$  deals with the reference path shape: it imposes that path and robot curvatures are equal. As the future curvature of the path to be followed can be known, as well as steering actuator features, a model predictive algorithm can be derived: the value of  $\delta_{Traj}$  (called  $\delta_{Traj}^{Pred}$  in the sequel) to be applied at the current time, to reach "at best" the future curvature on a fixed horizon of prediction, is then computed. This optimal term is then substituted to term  $\delta_{Traj}$ , so that the adaptive and predictive control law is finally:

$$\delta_F = \delta_{Traj}^{Pred} + \delta_{Deviation} \quad (9)$$

### 2.4. Limitations

The above described path tracking algorithm is attractive since the results obtained during full scale experiments show very small tracking errors (see for instance [7]: the guidance accuracy stays within a range of  $\pm 10$ cm whatever the shape of the path and terrain conditions (geometry and grip conditions)). Nevertheless, these satisfactory results have been obtained at limited speed (below 2m/s) and simulations as well as experiments highlight that an increase in velocity may reduce the efficiency of this approach. In particular, oscillations at transient phases tend to appear at high speed (above 4 m/s), depreciating the overall closed-loop behavior.

These drawbacks are mainly due to the preliminary sideslip angle observer (5). As it is based only on an

extended kinematic representation, this estimation does not take into account any equation describing sideslip angle time-evolution (only available in dynamic representations), and in particular the link with the measured steering angle. As a result, the estimation of such variables is necessarily delayed. A new observer is then designed, relying on both dynamic equations (to increase reactivity) and kinematic representation (to avoid the knowledge of numerous dynamic parameters).

### 3. Mixed kinematic/dynamic Observer design

#### 3.1. General algorithm description

In order to rely on dynamic models, the knowledge of the parameters describing grip conditions are mandatory. These parameters are however varying with the soil nature and cannot be measured directly. Nevertheless, the preliminary observer, based on the extended kinematic model, is able to supply delayed informations, which can be used for the estimation of slow-varying terrain properties. The proposed observer then takes part of the complementarity between extended kinematic and dynamic models, as it is described on Figure 2.

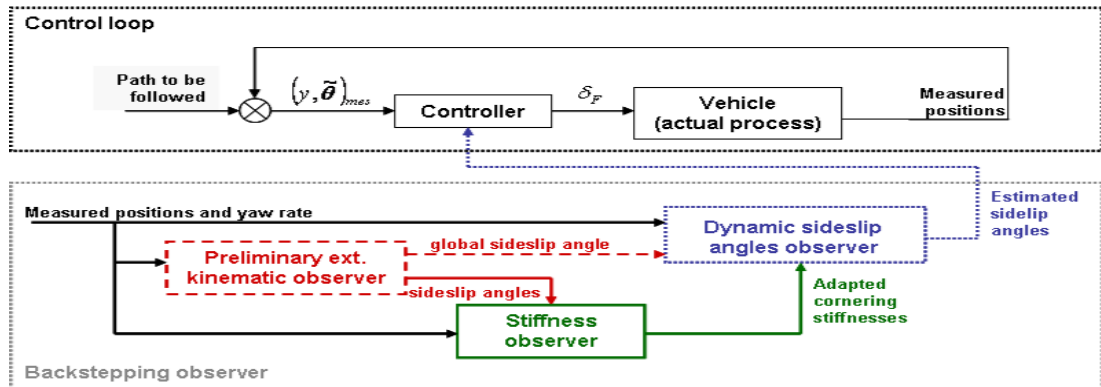


Figure 2: Observer principle scheme

In a first step, the preliminary observer (depicted in red/dashed box) permits to extract a first estimation of sideslip angles, considered accurate enough to estimate slow-varying parameters. Using this knowledge, grip conditions are then estimated via the adaptation of cornering stiffnesses (hereafter denoted by  $C_F$  and  $C_R$ , see the definition in equation (10)). This second step, depicted as the green/dotted box in Figure 2, permits to feed a simplified dynamic model (together with known and invariant parameters: mass, inertia and center of gravity position). Finally, this known dynamic model is used to derive a sideslip angle observer taking explicitly into account dynamic effects (blue/dashed dotted box). Each of these steps is detailed below, after introducing the partial dynamic model acting together with the extended kinematic one.

#### 3.2. Dynamic model

As achieved in [5], robot motion is described in the yaw frame (as depicted in Figure 3), still considering the robot as a bicycle. In this representation, only lateral forces are accounted, assuming that the vehicle velocity is slow-varying. The additional required notations introduced with respect to the extended kinematic model are:

- $G$  is the vehicle center of gravity,
- $a$  and  $b$  are respectively the front and rear half-wheelbases,
- $u$  is the linear velocity at the center of gravity,
- $\beta$  is the vehicle global sideslip angle,
- $F_f$  and  $F_r$  are respectively the lateral forces generated at the front and rear tires.
- $m$  is the total mobile robot mass.
- $I_z$  is the moment of inertia along the vertical axis.

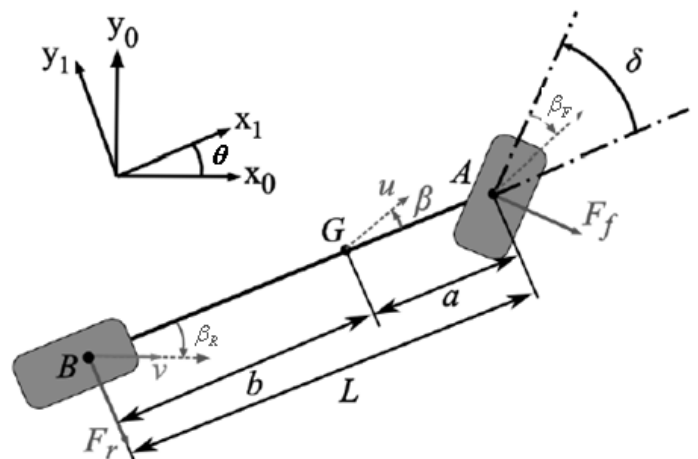


Figure 3: Dynamic bicycle model with sliding parameters.

A dynamic model can then be derived from Euler-Lagrange equations, linking acceleration to lateral forces  $F_f$  and  $F_r$ . Basically, these forces are non-linear functions of sideslip angles (see for example [3]). In on-road applications, a linear approximation can be assumed (the linear proportionality coefficient is

then called tire cornering stiffness). In contrast, in an off-road context, such an approximation is no longer valid. However, in order to reduce the number of parameters, a linear relationship is here considered, but with a slow-varying stiffness (as achieved in [1]):

$$\begin{cases} F_f = C_F(\cdot)\beta_F \\ F_r = C_R(\cdot)\beta_R \end{cases} \quad (10)$$

The knowledge of  $C_F$  and  $C_R$  is assumed to be known via the cornering stiffnesses adaptation detailed hereafter.

Since non-linear tire behavior has been described via cornering stiffness adaptation, and since sideslip angles (front, rear, and global ones) are quite small in practice, mobile robot dynamic equations can be linearized around null sideslip angles, leading to the dynamic model to be considered in the sequel:

$$\begin{cases} \dot{\theta} = \frac{1}{I_z} (-aC_F\beta_F \cos(\delta_F) + bC_R\beta_R) \\ \dot{\beta} = -\frac{1}{um} (C_F\beta_F \cos(\delta_F) + C_R\beta_R) - \dot{\theta} \\ \beta_R = \beta - \frac{b\dot{\theta}}{u} \\ \beta_F = \beta + \frac{a\dot{\theta}}{u} - \delta_F \\ u = v \end{cases} \quad (11)$$

### 3.3. Tire cornering stiffness adaptation

The objective of this observer is to estimate the two cornering stiffnesses  $C_F$  and  $C_R$  representative of grip conditions. As  $C_F$  and  $C_R$  are expected to be slow-varying, the preliminary sideslip angles observer (5) can be seen as a reference for the observer to be designed. Let us denote  $\beta_F$  and  $\beta_R$ , the estimated variables supplied by observer (5). An estimation of the global sideslip angle, denoted  $\beta$ , can then be immediately inferred from model (11):

$$\bar{\beta} = \frac{b\bar{\beta}_F + a\bar{\beta}_R + b\delta_F}{L} \quad (12)$$

Let  $X_1 = [\dot{\theta} \ \bar{\beta}]^T$  be the observed state and  $u = [C_F \ C_R]^T$  the control vector. Equations (11) can then be rewritten as the following state space form:

$$\dot{X}_1 = A_1 X_1 + B_1 u \quad (13)$$

where:

$$A_1 = \begin{bmatrix} 0 & 0 \\ -1 & 0 \end{bmatrix}, \quad B_1 = \begin{bmatrix} -\frac{a\bar{\beta}_F \cos(\delta_F)}{I_z} & \frac{b\bar{\beta}_R}{I_z} \\ -\frac{\bar{\beta}_F \cos(\delta_F)}{um} & -\frac{\bar{\beta}_R}{um} \end{bmatrix} \quad (14)$$

Cornering stiffnesses are here viewed as control variables to be designed to ensure the convergence of  $X_1$  to the measured state  $X = [\dot{\theta} \ \beta]^T$ , where  $\dot{\theta}$  is the measured yaw rate and  $\beta$  is given by (12). Let  $\epsilon_X = X_1 - X$  denote the observer error. Then, the following expression for  $u$ :

$$u = B_1^{-1} [G_1 \epsilon_X + \dot{X} - A X_1] \quad (15)$$

leads to:

$$\dot{\epsilon}_X = G_1 \epsilon_X \quad (16)$$

where  $G_1$  is a positive definite matrix, so that exponential convergence of  $X_1$  to the measured yaw rate and preliminary estimated global sideslip angle is ensured.

Expression (15) constitutes therefore a relevant adaptation of cornering stiffnesses, ensuring that dynamic model (11) is reliable as soon as  $B_1$  is invertible. The invertibility condition of this matrix also constitutes the observability condition of cornering stiffnesses estimation. As can be observed in (14),  $B_1$  is singular when sideslip angles are null, and badly conditioned when sideslip angles are close to 0. Such cases occur when mobile robots move according to a straight line on an even ground, which is a quite standard situation. Therefore, in the sequel, the conditioning of matrix  $B_1$  is tested prior to activate cornering stiffness estimation and freezes adaptation of  $C_F$  and  $C_R$  to previous values if conditioning is unsatisfactory.

### 3.4. Dynamic sideslip angle estimation

Since relevant estimations of  $C_R$  and  $C_F$  are supplied on-line by observer (15), all parameters in dynamic model (11) are now known. Standard observer theory can then be applied to this model. Since dynamic effects are described in model (11), it is expected that this second sideslip angle observer presents a higher reactivity than observer (5), previously built from extended kinematic model (1).

Let us first inject the third and fourth equations in (11) into the first two ones. Dynamic model (11) can then be presented as a linear state space form, with  $X_2 = [\dot{\theta} \ \beta]^T$  as state vector and  $\delta_F$  as control variable:

$$\dot{X}_2 = A_2 X_2 + B_2 \delta_F \quad (17)$$

where:

$$A_2 = \begin{bmatrix} \frac{-a^2 C_F - b^2 C_R}{u I_x} & \frac{-a C_F + b C_R}{I_x} \\ -\frac{a C_F - b C_R}{u^2 m} - 1 & -\frac{C_F + C_R}{u m} \end{bmatrix}, \quad B_2 = \begin{bmatrix} \frac{a C_F}{I_x} \\ \frac{C_F}{u m} \end{bmatrix} \quad (18)$$

(it has also been assumed that  $\cos \delta_F \approx 1$ )

The standard observer equation associated with model (17) is:

$$\dot{\hat{X}}_2 = A_2 \hat{X}_2 + B_2 \delta_F + G_2 \bar{X}_2 \quad (19)$$

where  $\hat{X}_2 = [\hat{\theta}_2 \ \hat{\beta}_2]^T$  is the observed state,  $X = [\dot{\theta} \ \beta]^T$  is the measured state (measured yaw rate and preliminary global sideslip angle estimation (12)) and  $\bar{X}_2 = \hat{X}_2 - X$  is the observer error. From (17) and (19), it can be deduced that:

$$\dot{\bar{X}}_2 = (A_2 + G_2) \bar{X}_2 \quad (20)$$

Convergence of the observer error  $\bar{X}_2$  to zero is then ensured, provided that  $G_2$  is chosen such that  $A_2 + G_2$  is negative definite.  $\beta$  has been chosen as the measurement associated with the observed state  $\hat{\beta}_2$ , since its steady state value is always correct. Nevertheless, since  $\beta$  values are no longer accurate during transient phases, preference should be given to the convergence of  $\hat{\theta}_2$  (since yaw rate measurement is reliable) with respect to the convergence of  $\hat{\beta}_2$ . This can easily be imposed by tuning  $G_2$  such that the settling time associated with  $\hat{\theta}_2$  is shorter than the one associated with  $\hat{\beta}_2$ .

Finally, the front and rear sideslip angles to be used in control law (9) can be obtained by injecting  $\hat{\beta}_2$  into the third and fourth equations in (11):

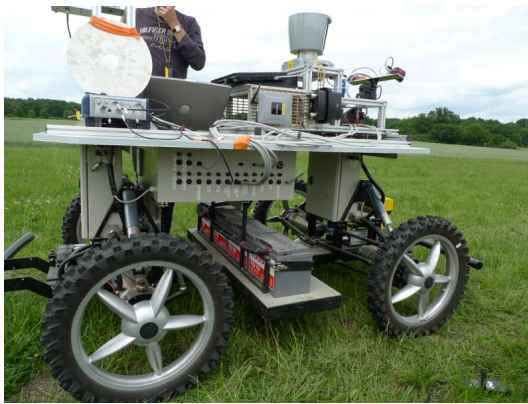
$$\begin{cases} \hat{\beta}_R = \hat{\beta}_2 - \frac{b \dot{\theta}}{u} \\ \hat{\beta}_F = \hat{\beta}_2 + \frac{a \dot{\theta}}{u} - \delta_F \end{cases} \quad (21)$$

Equations (21) constitute the mixed kinematic and dynamic sideslip angle observer. As demonstrated below, when off-road mobile robots move at high speed, observer (21) permits, with respect to observer (5), to improve the robustness and the reactivity of sideslip angle estimation, and therefore the performances of path tracking.

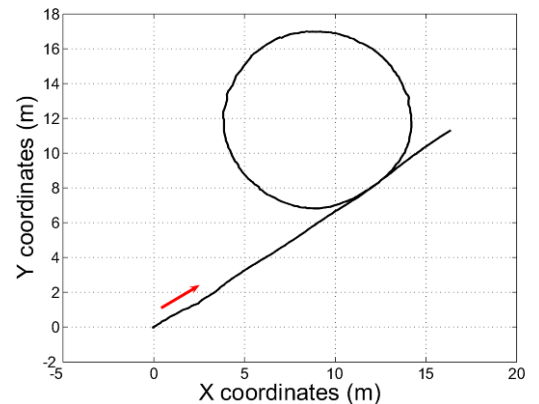
## 4. EXPERIMENTAL RESULTS

### 4.1. Experimental set-up

The experimental platform used to validate the proposed approach is shown in Figure 4(a). It consists in a fully electric off-road mobile robot with four steering wheels. Its weight and maximum speed are respectively 600kg and 2.5m/s. The main exteroceptive sensor on-board is an RTK-GPS receiver, that can supply an absolute position accurate to within 2cm, at a 10Hz sampling frequency. The GPS antenna has been located straight up the center of the rear axle, so that the absolute position of point  $R$  (i.e. the point to be controlled, see Figures 1 and 3) is straightforwardly obtained from the sensor. In addition, a gyrometer supplying a yaw rate measurement accurate to within 0.1°/s has been settled on the chassis, to provide cornering stiffness observer (15) and dynamic sideslip angle observer (21) with this information. The dynamic properties of the mobile robot are reported on table IV-A



(a) Experimental platform



(b) Reference trajectory

Figure 4: Experimental robot and desired path

The proposed observer has been validated via actual automated path tracking. The reference path is shown on Figure 4(b). Capabilities have been investigated by achieving the three following tests:

- Test 1: Classical path tracking. In this test, wheel slippage is neglected (i.e.  $(\beta_F, \beta_R) = (0,0)$  is entered into control (9)). Results of this test are depicted in black plain line in the following figures.

- Test 2: Path tracking using preliminary sideslip angle observer. This test has been carried out when using  $\beta_F$  and  $\beta_R$  supplied by (5) into control law (9). Results of this test are depicted in red dotted line in the following figures.
- Test 3: Path tracking using mixed kinematic and dynamic sideslip angle observer. This test has been carried out when using  $\hat{\beta}_F$  and  $\hat{\beta}_R$  supplied by (21) into control law (9). Results of this test are depicted in magenta dashed line in the following figures.

These three tests have been performed on a terrain composed of wet grass (low grip conditions) at a 2.5m/s velocity (maximum velocity available with the robot actuators).

Mass	$m = 675\text{kg}$
Vertical inertia	$I_z = 310\text{kg.m}^2$
Front half wheelbase	$a = 0.72\text{m}$
Rear half wheelbase	$b = 0.5\text{m}$

Table I: Experimental robot dynamic parameters

### 5. Path tracking results

Path tracking errors (i.e. lateral deviations with respect to the reference path) are compared in Figure 5. First of all, the result related to Test 1 shows clearly the importance to account for sliding: the lateral deviation is quite small during the straight line part of the reference path (from  $t=0$  to  $t=10\text{s}$ ), but a constant and significant error is recorded when the robot enters into the curve (up to 50cm). On the contrary, both tracking errors obtained with a control law accounting for sliding (Tests 2 and 3) present a null lateral deviation during curves. Nevertheless, the impact of the delay in sideslip angle estimation on guidance accuracy can be observed. In Test 2, when sliding variables are estimated from an extended kinematic model, a non-negligible overshoot (around 40cm) is recorded at the beginning of the curve (at  $t=14\text{s}$ ). The reactivity of the proposed observer, relying on a dynamic model, permits to decrease this overshoot: in Test 3, the maximum deviation at  $t=14\text{s}$  is only 20cm and path tracking is accurate within  $\pm 10\text{cm}$  almost all the path long.

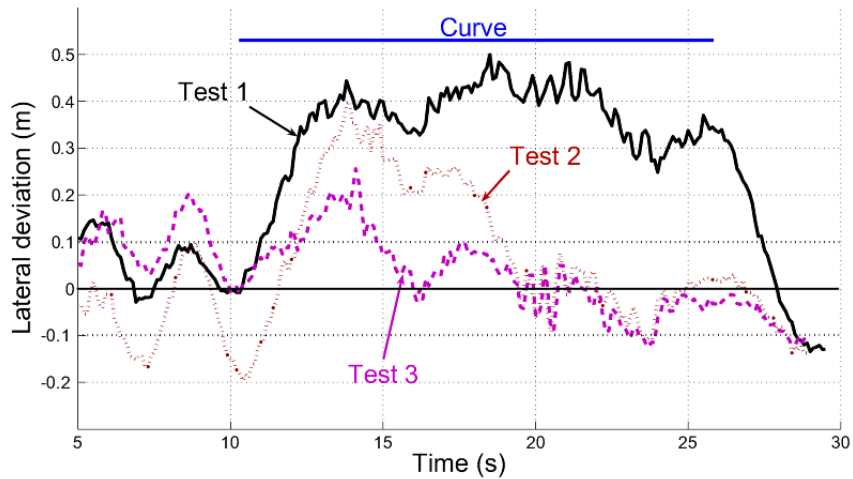


Figure 5: Comparison of obtained path tracking errors

The faster sideslip estimation is highlighted in Figure 6(a). The front sideslip angle estimation recorded during Test 2 and Test 3 are well superposed before the curve (before 10s) and during steady state phases (between 19s and 25s - end of the curve). In contrast, at transient phases (between 10 and 19s and after 25s), the estimation obtained with the dynamic observer reacts prior to the estimation supplied by the extended kinematic observer. Moreover, an higher absolute value is provided just before steady state phases. This higher reactivity explains the improvement in the mobile robot behavior pointed out in Figure 5, and shows the efficiency of the proposed observer.

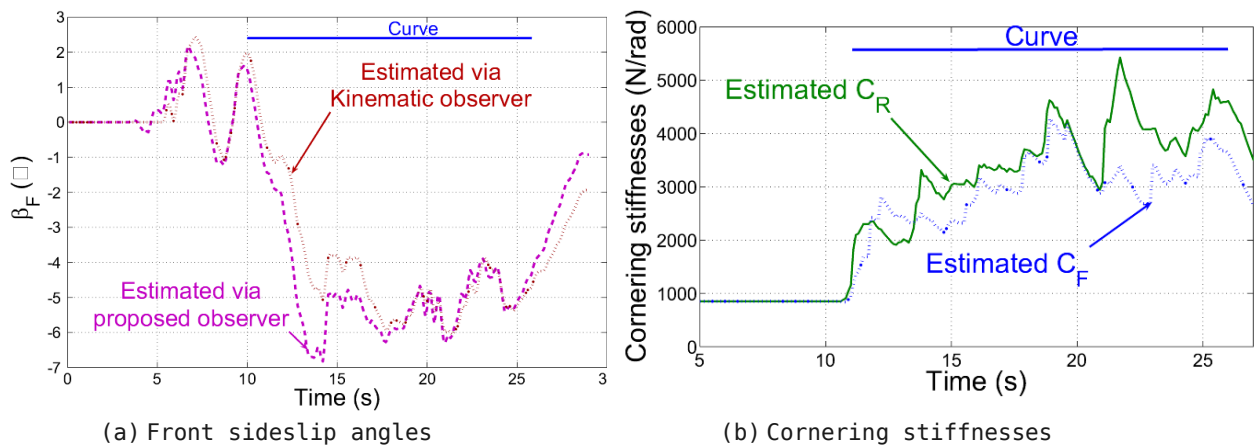


Figure 6: Results on observed variables

The proposed dynamic observer relies on cornering stiffness adaptation (15), devoted to grip condition estimation, ensuring that dynamic model (11) is always relevant. The front and rear stiffness estimation during Test 3 is reported in Figure 6(b). It can be noticed that during the straight line part of the reference path (i.e. before  $t=10$ s) the adaptation is disabled (since cornering stiffnesses are not observable). During the curve, the adaptation is activated and permits to account for grip condition variation and non-linearity.

## 6. Conclusion and future work

This paper proposes a sideslip angle observer based on both dynamic and kinematic models to enable automated path tracking for fast off-road mobile robots. The use of a multi-model approach permits to reduce the estimation delay (as it accounts for robot high dynamics) while avoiding the knowledge of numerous parameters (as extended kinematic representation permits to adapt on-line dynamic parameters, mainly cornering stiffnesses). This approach is particularly suitable for off-road mobile robots, since the knowledge of variable grip conditions is mandatory for the design of an accurate control law (within several centimeters). The reactivity obtained with this approach allows to investigate high speed control. Capabilities of such an innovative observer have been compared to those of a purely extended kinematic approach through experimental tests. They show the improved reactivity and the relevance of the estimated signals, since the tracking error recorded during transient phases is drastically reduced, leading to a path tracking accuracy within  $\pm 10$ cm almost all time long, whatever the velocity level, the grip conditions and the shape of the desired trajectory. The good results obtained in experiments have been tested at higher speed (up to 8 m/s) through advanced simulations (using Adams and Simulink softwares). They show the relevance of the approach at these velocity levels. Additional experimental tests using a faster mobile robot are expected to corroborate simulation results. In addition, the new data supplied by the proposed observer on the grip conditions (mainly cornering stiffnesses), also permit to feed a control law dedicated to the robot integrity (mainly stability control in a sense of rollover and overturn).

## 7. References

- [1] N. Bouton, R. Lenain, B. Thuilot, and P. Martinet, *Backstepping observer dedicated to tire cornering stiffness estimation: Application to an all terrain vehicle and a farm tractor*, IEEE/RSJ International Conference on Intelligent RObots and Systems IROS2007 (San Diego, CA, USA), 2007, pp. 1763–1768.
- [2] J. Bruinsma, *World agriculture: Towards 2015/2030. An FAO perspective.*, Tech. report, Food and Agriculture Organisation, 2003.
- [3] C. Canudas de Wit, H. Olsson, K.J. Astrom, and P. Lischinsky, *A new model for control of systems with friction*, IEEE Transactions on Automatic Control **40** (1995), no. 3, 419–425.
- [4] R. Eaton, J. Katupitiya, K. W. Siew, and K. S. Dang, *Precision guidance of agricultural tractors for autonomous farming*, 2nd Annual IEEE Systems Conference, 2008, 2008, pp. 1–8.
- [5] M. Ellouze and B. d'Andréa-Novel, *Control of unicycle-type robots in the presence of sliding effects with only absolute longitudinal and yaw velocities measurement.*, European Journal of Control **6** (2000), no. 6, 567–584.
- [6] F. Hao, R. Lenain, B. Thuilot, and P. Martinet, *Robust adaptive control of automatic guidance of farm vehicles in the presence of sliding*, IEEE International Conference on Robotics and Automation (ICRA) (Barcelona (Spain)), 2005, pp. 3113–3118.
- [7] R. Lenain, B. Thuilot, C. Cariou, and P. Martinet, *Adaptive and predictive path tracking control for off-road mobile robots*, European Journal of Control **13** (2007), no. 4, 419–439.
- [8] E. Lucet, C. Grand, D. Salle, and P. Bidaud, *Stabilization algorithm for a high speed car-like robot achieving steering maneuver*, IEEE International Conference on Robotics and Automation (ICRA)

(Pasadena, CA, USA.), 2008, pp. 2540–2545.

[9] B. Martin, K Iagnemma, and S. Sanjiv, *The 2005 darpa grand challenge: The great robot race*, Springer Tracts in Advanced Robotics **36** (2007).

[10] A. Micaelli and C. Samson, *Trajectory tracking for unicycle-type and two-steering-wheels mobile robots*, INRIA technical report (1993), no. N 2097.

[11] C. Samson, *Control of chained systems. application to path following and time-varying point stabilization of mobile robots*, IEEE Transactions on Automatic Control **40(1)** (1995), 64–77.

[12] S. Scheding, G. Dissanayake, E. Nebot, and H. Durrant-Whyte, *Slip modeling and aided inertial navigation of an lhd*, Proceedings of the IEEE Int. Conf. on Robotics and Automation (Albuquerque, New Mexico, USA), 1997, pp. 1904–1909.

[13] R. Siegwart and I. R. Nourbakhsh, *Introduction to autonomous mobile robots*, MIT Press, 2004., 2004.

[14] D. Wang and C.B. Low, *An analysis of wheeled mobile robots in the presence of skidding and slipping: Control design perspective*, IEEE International Conference on Robotics and Automation (ICRA) (Roma, Italy), 2007, pp. 2379–2384.